From Granger causality to long-term causality: Application to climatic data

Dmitry A. Smirnov[1,*] and Igor I. Mokhov[2,†]
[1]*Saratov Branch of V. A. Kotel'nikov Institute of Radio Engineering and Electronics, Russian Academy of Sciences, 38 Zelyonaya Street, Saratov 410019, Russia*
[2]*A. M. Obukhov Institute of Atmospheric Physics, Russian Academy of Sciences, 3 Pyzhevsky, Moscow 119017, Russia*
(Received 24 November 2008; revised manuscript received 11 February 2009; published 14 July 2009)

Quantitative characterization of interaction between processes from time series is often required in different fields of natural science including geophysics and biophysics. Typically, one estimates "short-term" influences, e.g., the widely used Granger causality is defined via one-step-ahead predictions. Such an approach does not reveal how strongly the "long-term" behavior of one process under study is affected by the others. To overcome this problem, we introduce the concept of long-term causality, which extends the concept of Granger causality. The long-term causality is estimated from data via empirical modeling and analysis of model dynamics under different conditions. Apart from mathematical examples, we apply both approaches to find out how strongly the global surface temperature (GST) is affected by variations in carbon dioxide atmospheric content, solar activity, and volcanic activity during the last 150 years. Influences of all the three factors on GST are detected with the Granger causality. However, the long-term causality shows that the rise in GST during the last decades can be explained only if the anthropogenic factor (CO_2) is taken into account in a model.

DOI: 10.1103/PhysRevE.80.016208 PACS number(s): 05.45.Tp, 92.70.Mn, 02.50.Sk, 02.50.Tt

I. INTRODUCTION

The problem of detection and quantitative characterization of couplings between complex processes from observed time series arises in multiple fields including physics [1,2], geophysics [3–11], and neurophysiology [12–30]. Numerous investigations are devoted to synchronization which is an effect of interaction observed in ensembles of nonlinear systems (e.g., [1,4,7,13,17,24,31,32]). In the last decade, a closer attention is paid to the analysis of directional couplings.

Apart from traditional cross-correlation functions, cross-spectral analysis, and multivariate linear autoregressive models [3,9,11,23,30,33], various techniques are developed in the framework of nonlinear dynamics. Thus, synchronization indices quantify interdependence between simultaneous states of the systems under investigation (e.g., [1,17,31]). Similar asymmetric measures are based on mutual nonlinear prediction [14,16], recurrence plots [34], and nearest-neighbors statistics [15,24,35,36]. However, these asymmetric measures can reveal directional couplings (causal influences) only under additional assumptions (e.g., [15,34]). Transfer entropy [37] and Granger causality [33] are more appropriate and "direct" approaches to detect an influence of a process $y(t)$ on a process $x(t)$. Transfer entropy is based on the information-theoretic formalism and defined via probability density function for the nearest future of $x(t)$ conditioned to the present states of x and y, (see also [6,38,39]). The widely used Granger causality is based on linear [33] or nonlinear [40,41] empirical models and defined via one-step-ahead prediction improvement for the process x, which is achieved if the process y is taken into account in a model.

Both approaches are successfully used to detect directional couplings and quantify their *short-term* effects. However, it is often more important to learn how *long-term* characteristics of a process x (e.g., its power spectrum, amplitude of oscillations, trends, etc.) would change if a process y behaved in a certain way? Thus, in studying Parkinsonian tremor, one develops deep brain stimulation techniques [42] and reveals how the brain activity should be changed to provide a normal behavior of the limbs instead of their pathological high-amplitude oscillations. Another example is the question about the causes of contemporary global warming, which is widely debated in climatology [6,11,43]. Has the global surface temperature (GST) increased by three quarters of a degree over the last century due to anthropogenic factors, natural factors, or their combination? Both problems relate to the characterization of long-term effects of couplings between the processes.

As a tool for such a characterization, we suggest an idea of the long-term causality, which complements the Granger causality concept. The paper is organized as follows. We discuss the Granger causality estimation in Sec. II A and troubles in its interpretation in Sec. II B. The long-term causality is described and illustrated in Sec. III. Influences of three factors (solar activity, volcanic activity, and carbon dioxide atmospheric content) on the GST are analyzed with both approaches in Sec. IV. We summarize in Sec. V.

II. GRANGER CAUSALITY

The problem is commonly formulated as follows. There are time series from M processes $\{x_k(t)\}_{t=1}^{N}$, $k=1,\ldots,M$, where N is a time series length and sampling interval is set equal to unity. It is necessary to reveal and characterize couplings between the processes, i.e., to find out how they influence each other.

A. Description of the method

In case of two linear processes [20,33], one first constructs univariate autoregressive (AR) models

*smirnovda@info.sgu.ru
†mokhov@ifaran.ru

$$x_k(t) = A_{k,0} + \sum_{i=1}^{d} A_{k,i} x_k(t-i) + \xi_k(t), \quad k = 1,2, \tag{1}$$

where d is a model order, ξ_k are Gaussian white noises with variances $\sigma^2_{\xi_k}$. We denote the vector of coefficients $\mathbf{A}_k = \{A_{k,i}, i=0,\ldots,d\}$, the sum of squared residual errors $\Sigma^2_k = \Sigma_{t=d+1}^{N} [x_k(t) - A_{k,0} - \Sigma_{i=1}^{d} A_{k,i} x_k(t-i)]^2$, and its minimal value $s_k = \min_{\mathbf{A}_k} \Sigma^2_k$. The coefficients are estimated via the least-squares routine: $\hat{\mathbf{A}}_k = \arg\min_{\mathbf{A}_k} \Sigma^2_k$. An unbiased estimator for $\sigma^2_{\xi_k}$ which represents the mean-squared prediction error of the univariate model is given by $\hat{\sigma}^2_k = \frac{s^2_k}{N-d-(d+1)}$, where $d+1$ is the number of estimated coefficients in the model equation. The model order d is selected large enough to provide uncorrelatedness of the residual errors. To determine the necessary value of d automatically, one often uses criteria of Akaike [44] or Schwartz [45].

Then, one similarly constructs a bivariate AR model,

$$x_k(t) = a_{k,0} + \sum_{i=1}^{d} [a_{k,i} x_k(t-i) + b_{k,i} x_j(t-i)] + \eta_k(t), \tag{2}$$

where $j,k=1,2$, $j \neq k$, η_k are Gaussian white noises. Minimal values of the sums of squared residual errors are denoted $s^2_{1|2}$ and $s^2_{2|1}$ for the first and second processes, respectively. Unbiased estimators for the residual error variances are denoted $\hat{\sigma}^2_{1|2}$ and $\hat{\sigma}^2_{2|1}$. Prediction improvement for the process x_k achieved with the model (2) as compared to the model (1) characterizes the influence of x_j on x_k $(j \to k)$: $G_{j\to k} = \hat{\sigma}^2_k - \hat{\sigma}^2_{k|j}$.

We note that the value of $G_{j\to k}$ is an estimate obtained from a time series. In a definition of a theoretical (true) prediction improvement $G^{true}_{j\to k}$, one minimizes the expectation of the squared prediction error instead of the empirical sum Σ^2_k to determine the values of model coefficients, i.e., one uses ensemble averaging or averaging over an infinitely long realization instead of averaging over a finite time series. Thus, $G^{true}_{j\to k} = 0$ for uncoupled processes x_1 and x_2, but the estimator $G_{j\to k}$ can take on positive values just due to random fluctuations. Therefore, one needs a criterion to decide whether an obtained positive value of $G_{j\to k}$ implies the presence of the influence $j \to k$. It can be shown that the quantity $F_{j\to k} = \frac{(N-3d-1)(s^2_k - s^2_{k|j})}{s^2_{k|j} d}$ is distributed according to Fisher's F law with $(d, N-3d-1)$ degrees of freedom. Therefore, one can conclude that $G^{true}_{j\to k} > 0$, i.e., the influence $j \to k$ exists, at a significance level p if $F_{j\to k}$ exceeds $(1-p)$ quantile of the respective F distribution. It is called the F test or Granger and Sargent test (e.g., [38]).

If a time series is short, it is problematic to use high values of d since a large number of estimated coefficients can then lead to insignificant conclusions about coupling presence. The difficulty can be overcome in part if one constructs a bivariate AR model in the form,

$$x_k(t) = a_{k,0} + \sum_{i=1}^{d_k} a_{k,i} x_k(t-i) + \sum_{i=1}^{d_{j\to k}} b_{k,i} x_j(t-i-\Delta_{j\to k}) + \xi_k(t), \tag{3}$$

where $j,k=1,2$, $j \neq k$, and one selects a separate univariate model order d_k for each process instead of a common d in Eq. (1), a separate value of $d_{j\to k}$, and a separate trial delay time $\Delta_{j\to k}$. If at least some of the values d_k and $d_{j\to k}$ can be made small then the number of estimated coefficients is reduced.

If one needs nonlinear models, the difficulty gets even harder due to the "curse of dimensionality." In a nonlinear case, the procedure of coupling estimation remains the same but the AR models involve nonlinear functions. For instance, one may use univariate models,

$$x_k(t) = f_k(x_k(t-1), \ldots, x_k(t-d_k), \mathbf{A}_k) + \eta_k(t), \tag{4}$$

where f_k is a polynomial of some order P_k, and similar bivariate models. Apart from d_k and $d_{j\to k}$, it is important to choose the form of nonlinear functions properly. Polynomials [8], radial basis functions [40], and locally constant predictors [41] have been used. Yet, there is no regular procedure assuring an appropriate choice.

If the number of processes $M > 2$, then the estimation of the influence $j \to k$ can be performed in two ways:

(i) Bivariate analysis of x_j and x_k results in an estimator which reflects both a direct influence and that mediated by other observed processes.

(ii) Multivariate analysis takes into account all the M processes and allows to distinguish between the influences of different processes on x_k. Namely, one computes the squared prediction error for a multivariate AR model involving all the processes except for x_j and for a multivariate AR model involving all the M processes including x_j. If predictions are more accurate in the latter case, one infers the presence of the direct influence $j \to k$.

To express prediction improvements in relative units, one normalizes $G_{j\to k}$ by the variance $\hat{\sigma}^2_{x_k}$ of the process x_k or by the variance $\hat{\sigma}^2_k$ of the prediction error of a univariate model (1). The quantity $G_{j\to k}/\hat{\sigma}^2_k$ is used more often than $G_{j\to k}/\hat{\sigma}^2_{x_k}$. Both quantities are not greater than 1 and one may hope to give them a vivid interpretation. Thus, $G_{j\to k}/\hat{\sigma}^2_k$ is close to 1 if the influence $j \to k$ describes almost entirely the random term ξ_k unexplained by the univariate model (1). $G_{j\to k}/\hat{\sigma}^2_{x_k}$ is close to 1 if, in addition, the univariate model (1) explains a negligible part of the variance of x_k. However, these attempts of interpretation are often insufficient to assess the importance of the influences as discussed below.

B. Difficulties of interpretation

The following examples illustrate that quantities based on $G^{true}_{j\to k}$ can hardly be understood from the physical point of view as the "strength" of the influence $j \to k$ or its "importance."

The *first* example is a linear process x_1 driven by a delta-correlated process x_2,

$$x_1(t) = \alpha x_1(t-1) + x_2(t-1),$$

$$x_2(t) = \xi(t), \tag{5}$$

where $\alpha = \sqrt{0.99}$ and $\xi(t)$ is Gaussian white noise. Due to the closeness of α to unity, the process x_1 exhibits alternating stochastic trends and a large autocorrelation time. The vari-

ance of x_1 is $\sigma^2_{x_1}=\sigma^2_\xi/(1-\alpha^2)$. An optimal univariate AR model of x_1 is linear with $d_1=1$ and gives a prediction error variance $\sigma^2_1=\sigma^2_\xi$. Since $\sigma^2_{1|2}=0$ for a respective bivariate AR model, the prediction improvement is $G^{true}_{2\to1}=\sigma^2_\xi$. Normalized characteristics are $G^{true}_{2\to1}/\sigma^2_{x_1}=1-\alpha^2=0.01$ and $G^{true}_{2\to1}/\sigma^2_1=1$.

The *second* example is a chaotic quadratic map driven by zero-mean delta-correlated noise x_2 [46],

$$x_1(t)=\lambda-x_1^2(t-1)+x_2(t-1),$$

$$x_2(t)=\xi(t), \tag{6}$$

where $\lambda=1.85$ and $\sigma^2_\xi=0.000\,1$. The variance of x_1 computed from a very long realization is $\sigma^2_{x_1}=1.36$. An optimal univariate AR model of x_1 is quadratic with $d_1=1$. The values of σ^2_1 and $G^{true}_{2\to1}$ are equal to σ^2_ξ. Hence, $G^{true}_{2\to1}/\sigma^2_{x_1}\ll1$ and $G^{true}_{2\to1}/\sigma^2_1=1$. An effect of x_2 on the basic statistical characteristics of x_1 is rather weak since the quadratic map demonstrates almost the same behavior at $\sigma^2_\xi=0$, e.g., its variance is $\sigma^2_{x_1}=1.32$.

Thus, in both examples $G^{true}_{2\to1}/\sigma^2_{x_1}$ is very small while $G^{true}_{2\to1}/\sigma^2_1$ is large. According to the first quantity, one should say that the influence $2\to1$ is quite weak in both cases. According to the second quantity, one should infer that the influence $2\to1$ is quite considerable and approximately "equally strong" in both cases. However, in the first example one would observe an equilibrium state of x_1 without the influence $2\to1$ instead of high-amplitude fluctuations with long autocorrelations, i.e., the influence is fundamentally important. In the second example, the influence $2\to1$ leads just to a relatively weak increase in x_1 amplitude.

The main features of the above behavior of x_1 (long autocorrelations and self-sustained chaotic dynamics) are determined by the individual properties of x_1 such as the term $\alpha x_1(t-1)$ in Eq. (5) and nonlinearity in Eq. (6). Quantitative contribution of the term x_2 to the equation for x_1 is small in both cases. However, troubles are also encountered if a process x_1 is individually white noise as illustrated with the *third* example, where x_1 is driven by a process x_2 which exhibits strong autocorrelations,

$$x_1(t)=x_2(t-1)+\xi_1(t),$$

$$x_2(t)=\alpha x_2(t-1)+\xi_2(t), \tag{7}$$

where $\alpha=\sqrt{0.99}$ and $\xi_k(t)$ are independent Gaussian white noises with $\sigma^2_{\xi_1}=\sigma^2_{\xi_2}=\sigma^2_\xi=0.01$. Here, $\sigma^2_{x_1}=\sigma^2_{\xi_1}+\frac{\sigma^2_{\xi_1}}{1-\alpha^2}=1.01$ and the variance of x_1 without the influence of x_2 would be $\sigma^2_{\xi_1}=0.01$, i.e., 101 times as small. Further, $\sigma^2_{1|2}=\sigma^2_{\xi_1}=0.01$. A univariate AR model for x_1 gives a small prediction error already for $d=1$ since it manages to describe autocorrelations in x_1 induced by x_2. Based on Eq. (7) and an approximately optimal univariate predictor given by $\langle x_1(t)|x_1(t-1)\rangle \approx \alpha x_1(t-1)$ where $\langle\cdot\rangle$ stands for expectation and the vertical line means conditioning, a univariate model prediction error can be estimated as

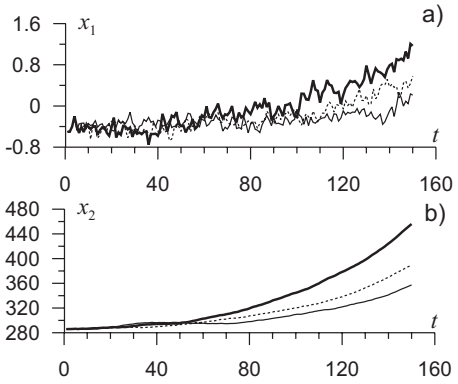

FIG. 1. Three time realizations of the system (8) selected randomly. Parameter values are obtained by fitting an AR model to climatic data for GST and CO_2 [Figs. 2(a) and 2(d)]: $\alpha_{1,0}=-1$, $\alpha_{1,1}=0.5$, $\alpha_{1,2}=\alpha_{1,3}=0$, $\alpha_{1,4}=0.2$, $\beta=0.003$, $\alpha_{2,0}=-2.456$, $\alpha_{2,1}=1.225\,6$, $\alpha_{2,2}=-0.295\,42$, $\alpha_{2,3}=0.285\,82$, $\alpha_{2,4}=0.091\,14$, $\alpha_{2,5}=-0.298\,49$, $\sigma^2_{\xi_1}=0.01$, and $\sigma^2_{\xi_2}=0.076\,6$. Initial conditions are the same for all realizations and also taken from the climatic data: $x_1(1)=-0.4$, $x_1(2)=-0.5$, $x_1(3)=-0.4$, $x_1(4)=-0.2$, $x_2(1)=285.8$, $x_2(2)=285.9$, $x_2(3)=286.0$, $x_2(4)=286.2$, and $x_2(5)=286.3$. The quantities x_1, x_2, and t are regarded dimensionless.

$$\begin{aligned}\varepsilon(t)&=\alpha x_1(t-1)-[x_2(t-1)+\xi_1(t)]\\&=\alpha[x_2(t-2)+\xi_1(t-1)]-[x_2(t-1)+\xi_1(t)]\\&=[\alpha x_2(t-2)-x_2(t-1)]+\alpha\xi_1(t-1)-\xi_1(t)\\&=-\xi_2(t-1)+\alpha\xi_1(t-1)-\xi_1(t)\end{aligned}$$

. Its variance is $\sigma^2_1=\sigma^2_\xi(2+\alpha^2)\approx2\sigma^2_\xi$. Hence, $G^{true}_{2\to1}\approx\sigma^2_\xi=0.01$ so that $G^{true}_{2\to1}/\sigma^2_{x_1}\ll1$ and $G^{true}_{2\to1}/\sigma^2_1\approx0.5$. Despite the influence $2\to1$ is rather strong and increases the variance of x_1 by two orders of magnitude, the value of $G^{true}_{2\to1}$ normalized in any way does not reflect this fact adequately. The reason is that the driving from x_2 is implicitly taken into account in a univariate model for x_1 so that the difference between univariate and bivariate model predictions is quite small.

The *fourth* example relates to nonstationary processes,

$$x_1(t)=\alpha_{1,0}+\sum_{i=1}^{4}\alpha_{1,i}x_1(t-i)+\beta x_2(t-1)+\xi_1(t),$$

$$x_2(t)=\alpha_{2,0}+\sum_{i=1}^{5}\alpha_{2,i}x_2(t-i)+\xi_2(t), \tag{8}$$

whose parameter values are selected so that their realizations mimic climatic time series for GST (x_1) and CO_2 atmospheric content (x_2) (Fig. 1). The driving process x_2 is nonstationary [Fig. 1(b)]. The driven process x_1 would be stationary for $\beta=0$ but gets nonstationary due to the nonstationary driving and also exhibits an increasing trend [Fig. 1(a)].

However, if the governing Eqs. (8) are not known *a priori*, one cannot confidently claim the presence of coupling just looking at the plots of $x_1(t)$ and $x_2(t)$. A trend similar to that observed in Fig. 1(a) may well be demonstrated by a stationary univariate AR process, e.g., by the process x_1 in

Eq. (5) and even by the process x_1 in Eq. (8) with $\beta=0$. These stationary processes demonstrate irregular alternation of intervals with increasing and decreasing trends which are called stochastic trends.

To detect the presence of the influence, one can use the Granger causality formalism with some peculiarities. Despite that stationarity of the processes is usually implied to define prediction improvement, one can define it in a similar way for nonstationary AR processes with constant parameters and stationary noises ξ_k [e.g., for Eqs. (8)]. First, for uncoupled nonstationary processes of such a type, residual errors of univariate and multivariate models are Gaussian and stationary since they represent the influence of stationary noises ξ_k. Thus, the F test is applicable to reject the hypothesis of uncoupled processes exactly as in the stationary case. Second, if the driving $j\to k$ is present, the meaning of the value $G_{j\to k}$ obtained as in Sec. II A somewhat differs from that for the stationary processes. In a nonstationary case, statistical properties of the prediction errors for any AR model are well defined under fixed initial conditions for all the processes under study. In particular, the mean-squared prediction error σ_k^2 for any univariate AR model depends on time since it is determined to a certain extent by the influence from a nonstationary process x_j. In contrast, the variance $\sigma_{k|j}^2$ is constant since it represents a stationary noise ξ_k. The difference $\sigma_k^2-\sigma_{k|j}^2$ at each time instant can be called a prediction improvement. It depends on time: $G_{j\to k}^{true}=G_{j\to k}^{true}(t)$. The quantity $G_{j\to k}$ defined in Sec. II A is an estimator for $\langle G_{j\to k}^{true}(t)\rangle_t$ averaged over the observation interval of the length N under given initial conditions. Hence, $G_{j\to k}$ systematically depends on the observation interval and initial conditions. In particular, it rises with expanding observation interval for the example (8). Moreover, since σ_k^2 and $\sigma_{x_k}^2$ depend on time for nonstationary processes, their estimators $\hat{\sigma}_{x_k}^2$ and $\hat{\sigma}_k^2$ should be also interpreted as the quantities related to specific initial conditions and observation interval.

For the example (8), we computed $\hat{\sigma}_{1|2}^2$ and $G_{2\to 1}$ for an observation interval $1\le t\le 150$ from an ensemble of 100 time series generated with the same initial conditions given in the caption of Fig. 1. As a result, the influence $2\to 1$ at a significance level $p=0.05$ is detected in 80 of the 100 cases. The influence $1\to 2$ is detected (erroneously) in four cases, i.e., less than 5% as expected for $p=0.05$. Thus, the Granger causality estimation properly reveals unidirectional coupling in the system (8).

An averaged value of $\hat{\sigma}_1^2$ appears equal to 0.0105. Thus, taking into account that $\sigma_{1|2}^2=0.010\,0$, we estimate G averaged over 150 time steps for the given initial conditions as $\langle G_{2\to 1}^{true}(t)\rangle_t\approx\hat{\sigma}_1^2-\sigma_{1|2}^2=0.000\,5>0$. An averaged normalized quantity $G_{2\to 1}/\hat{\sigma}_1^2$ appears equal to 0.06. In other words, predictions of x_1 are improved due to the knowledge of the process x_2 by about 6% as compared to a univariate model. Looking at a single pair of time series like those presented in Fig. 1, one may pose a question: is the rise in x_1 is caused by the driving from x_2? Indeed, x_1 increases by the value of about 0.8 over 150 time steps which is several times greater than the fluctuations of x_1 around its trend. Can such a significant rise be induced by x_2 if the relative prediction improvement is only 0.06? It may seem quite probable that the increase in x_1 is just a stochastic trend due to its own dynamics rather than due to the driving from x_2. This question cannot be answered with the aid of the Granger causality.

In general, both processes x_j and x_k may exhibit nontrivial individual dynamics such as self-sustained oscillations, long relaxation times, slow trends, etc. In practice, one may have to deal with all the highlighted factors leading to difficulties in the interpretation of G values. Above, we have shown theoretical expressions for the prediction improvements or their estimates from long time realizations or large ensembles. Hence, all the difficulties are not determined by data deficit or other technical problems. They are inherent to the Granger causality concept itself. Obviously, they inevitably emerge in the coupling estimation from a short time series.

To summarize, our examples show that the prediction improvement can hardly be interpreted directly as the influence strength or importance. It shows to what extent a forecast of one process gets better if another process is taken into account in a model, i.e., it directly reflects just an effect of a researcher's *prior knowledge* about another process. Yet, our consideration does not cancel the fact that the Granger causality estimation is a basic tool to *detect* causal influences. Below, we just complement it with an approach allowing to assess long-term effects of the influences.

III. LONG-TERM CAUSALITY

A. Description of the method

We propose to characterize the influence $j\to k$ by analyzing changes in the dynamics of x_k which would take place if the process x_j behaved in a certain way. To realize the idea, we proceed as follows.

(i) A characteristic $S(x_k)$ of the process x_k essential for a problem under study is selected. One may be interested in statistical properties such as the power within a certain frequency band, dynamical properties such as the largest Lyapunov exponent, or concrete values of x_k such as its mean value at a given time instant t, etc. Thus, for the analysis of the global warming, the values of GST in recent years (e.g., in 2005) and their trend (e.g., in 1985–2005) are important.

(ii) An ensemble of time realizations $x_k(t)$ is generated with a multivariate AR model like Eq. (3). Initial conditions $x_k(1),\ldots,x_k(d_k)$ for each realization are the same. They are set equal to the corresponding observed values of x_k. All the processes x_i, $i=1,\ldots,M$, $i\neq k$, are considered as external influences so that their experimentally observed time series $x_i(t)$ is used as inputs to the equation for x_k. We call these conditions "original" and denote them C_0.

(iii) Expectation of $S(x_k)$ is estimated via averaging over the ensemble. It is denoted $\langle S(x_k)|C_0\rangle$. If the model is adequate, its realizations $x_k(t)$ are on average close to the observed time series $x_k(t)$ and the value of $S(x_k)$ estimated from the observed data lies within the limits of probable values of $S(x_k)$ estimated from the model realizations.

(iv) An ensemble of artificial time realizations $x_j(t)$ satisfying a condition $C(x_j)$, which specifies the above-mentioned hypothetical behavior of x_j, is generated.

(v) An ensemble of model time realizations $x_k(t)$ is generated similarly to the step (ii) with the only difference that artificial time series $x_j(t)$ obtained at the step (iv) rather than the original data $x_j(t)$ are used as inputs to the AR model for x_k.

(vi) Expectation of $S(x_k)$ over the second ensemble is computed. We denote it $\langle S(x_k)|C(x_j)\rangle$.

(vii) Long-term effect of the influence $j\to k$ (a characteristic of long-term causality) is defined as

$$E_{j\to k}=\langle S(x_k)|C_0\rangle-\langle S(x_k)|C(x_j)\rangle. \tag{9}$$

It can be convenient also to normalize $E_{j\to k}$, e.g., $e_{j\to k}=|E_{j\to k}/\langle S(x_k)|C_0\rangle|$ for $\langle S(x_k)|C_0\rangle\neq 0$.

Both $S(x_k)$ and $C(x_j)$ can be chosen in different ways depending on the problem under study [47]. Further, $E_{j\to k}$ depends on the empirical model used. The latter must be adequate both under the condition C_0 and $C(x_j)$. This requirement is satisfied if orbits of the vector process $\{x_1(t),\ldots,x_M(t)\}$ under $C(x_j)$ do not leave a state space domain where they "live" under C_0. Otherwise, one should have prior reasons to assume model adequacy under $C(x_j)$, i.e., to extrapolate. For instance, one may assume global linearity or low-order polynomial nonlinearity of the processes.

The suggested approach provides coupling characteristics which make clear physical sense. It relies on the long-term description and, hence, extends the Granger causality concept based on the short-term predictions.

B. Illustrative examples

To illustrate the usefulness of the long-term causality, we compute it for the examples presented in Sec. II B. We select the variance of x_1 as the statistic of interest for the examples (5)–(7): $S(x_1)=\sigma^2_{x_1}$. To assess the importance of the influence $2\to 1$, we compare $S(x_1)$ under C_0 to $S(x_1)$ under the condition that the influence is absent, i.e., $C(x_2)$ can be formulated as $x_2=0$.

For the example (5), the long-term effect is $E_{2\to 1}=\langle\sigma^2_{x_1}|C_0\rangle-\langle\sigma^2_{x_1}|x_2=0\rangle=\frac{\sigma^2_\xi}{(1-\alpha^2)}-0=\frac{\sigma^2_\xi}{(1-\alpha^2)}$ and the normalized value $e_{2\to 1}=1$. These numbers are easily interpreted. The nonzero variance of x_1 is fully determined by the driving from x_2, i.e., the coupling is fundamentally important to observe any dynamics of x_1 different from an equilibrium state. For the example (6), $E_{2\to 1}=1.36-1.32=0.04$ and the relative long-term effect is $e_{2\to 1}=(1.36-1.32)/1.36=0.03$. In other words, the change in the variance of x_1 due to the influence of x_2 is weak (only about 3%), showing that this driving is not so important as in the previous example. Thus, the long-term causality allows to distinguish clearly between the two cases as distinct from the Granger causality.

For the example (7), $E_{2\to 1}=1.01-0.01=1$ and $e_{2\to 1}\approx 0.99$, i.e., 99% of the variance of x_1 is determined by the driving from x_2. At the same time, the values of $G^{true}_{2\to 1}$ normalized in different ways are small or moderate, even though the influence $2\to 1$ determines almost the entire behavior of x_1. Thus, the long-term analysis appears again much more appropriate to characterize the importance of the influence.

For the example (8), we define $S(x_1)=x_1(150)-x_1(1)$ and $C(x_2)$ as $x_2(t)=x_2(1)=285.8$ for all t. In such a way, we address the above question whether the trend in x_1 observed over 150 time steps is induced by the influence of x_2. Analysis of ensembles consisting of 100 time series gives $\langle S(x_1)|C_0\rangle\approx 0.8$ and $\langle S(x_1)|x_2(t)=285.8\rangle\approx 0$. Thus, the long-term effect is estimated as $E_{2\to 1}\approx 0.8$ and $e_{2\to 1}\approx 1$, i.e., the trend in x_1 is fully caused by the driving from x_2 despite the normalized prediction improvement $G^{true}_{2\to 1}/\sigma^2_1$ is only 0.06 which may seem a small number.

To summarize, the long-term causality makes clear sense and properly characterizes the importance of the influence $2\to 1$ for all the above examples.

IV. APPLICATION TO CLIMATIC DATA

A. Problem and data

A key global problem is to determine the relative role of natural and anthropogenic factors in climate variations. To predict the future climate change induced by anthropogenic forcing, one must learn how strongly different factors affect global climate characteristics. Thus, an impact of solar activity variations on GST is quantified in [10,11,48] via the analysis of reconstructions and measurement data. The authors note a variable character of the solar activity influence on GST and, in particular, its increase in the second half of the 20th century. Investigations of a 3D global climate model show that the solar activity can determine only a relatively small portion of the global warming observed in the last decades. Considerable influence of an anthropogenic factor on GST is noted in Ref. [6]. However, the question about the relative role of different factors is still not answered convincingly on the basis of the observational data analysis.

The data used in our investigation are plotted in Fig. 2. They include annual values T of the mean GST anomaly in 1856–2005, i.e., the GST difference from the mean value taken over the base period 1961–1990 [49]; reconstructions and measurements of solar irradiance I in 1856–2005 [50]; volcanic activity V in 1856–1999 [51]; and carbon dioxide atmospheric content n in 1856–2004 [52].

We construct univariate models for GST (Sec. IV B) and analyze influences of different factors with bivariate models (Secs. IV C–IV E) and multivariate models (Sec. IV F). Since the main question is about the causes of the GST increase, we use two appropriate characteristics as $S(T)$: (i) the value of T in 2005 denoted as T_{2005}; (ii) angular coefficient of a straight line approximating the temporal profile $T(t)$ over the interval 1985–2005 in the least-squares sense (a characteristic of the recent GST trend) denoted as $\alpha_{1985-2005}$. For the original GST data, these characteristics take on the values $T_{2005}=0.502$ K and $\hat{\alpha}_{1985-2005}=0.02$ K/year.

Models are fitted to the intervals $[1856-L]$ for different values of L. Thereby, we select time intervals where the influence of each factor on the GST is most pronounced and determine the smallest L allowing to detect this influence. The largest possible L is equal to 2005 if the variable V is not included into the analysis (Secs. IV B, IV C, and IV E). Otherwise, the largest possible L is 1999 since the data for $V(t)$ are available only up to 1999 and optimal AR models for GST involve the value of V without any time delay (Secs. IV D and IV F).

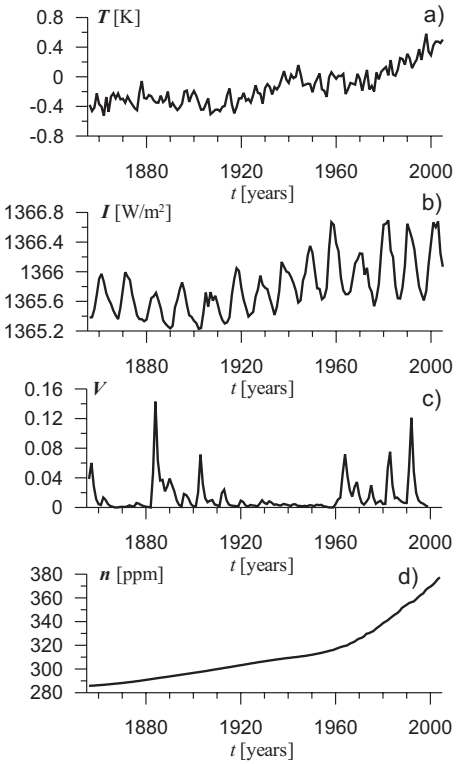

FIG. 2. The data used: (a) mean GST (its anomaly from the base period 1961–1990); (b) solar constant (irradiance in the range from infrared to ultraviolet wavelengths inclusively); (c) volcanic activity (optical depth of volcanic aerosol, dimensionless as discussed in [51]); (d) carbon dioxide atmospheric content in ppm.

B. Univariate models of GST variations

The mean-squared prediction error of a linear AR model (1) fitted to the interval [1856–2005] saturates at $d_T=4$ [Fig. 3(a)]. Incorporation of any nonlinear terms does not lead to statistically significant improvement (not shown). Thus, an optimal model reads as

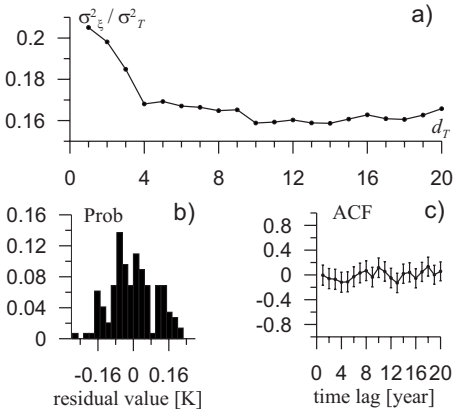

FIG. 3. Univariate modeling of GST (10): (a) normalized prediction error variance (dimensionless) versus model order (dimensionless); (b) histogram (dimensionless) of residual errors for $d_T=4$; (c) their autocorrelation function (dimensionless) with 95% confidence interval estimates

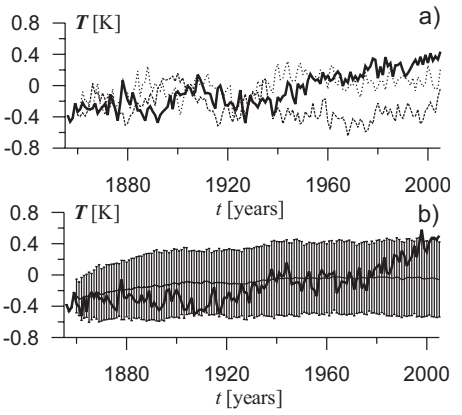

FIG. 4. Behavior of the model (10) fitted to the interval [1856–2005]: (a) three time realizations taken randomly from an ensemble of 100 realizations; (b) mean values over the ensemble (the thin line) and 95% intervals of the distributions (error bars) with the superimposed original data for GST (the thick line). Initial conditions are always set equal to the original GST values in 1856–1859.

$$T(t) = a_0 + \sum_{i=1}^{d_T} a_i T(t-i) + \xi(t), \tag{10}$$

where $d_T=4$, $a_0=-0.01\pm0.10$ K, $a_1=0.58\pm0.08$, $a_2=0.03\pm0.09$, $a_3=0.11\pm0.09$, and $a_4=0.29\pm0.08$. The intervals denote "± standard deviation estimate" coming from the least-squares routine. Prediction error variance is $\sigma_\xi^2=0.01$ K^2, while the sample variance of GST over the interval [1856–2005] is $\sigma_T^2=0.06$ K^2. In relative units $\sigma_\xi^2/\sigma_T^2=0.17$, i.e., 17% of the GST variance is not explained by the model. Residual errors for the model with $d_T=4$ look stationary (the plot is not shown) and do not exhibit signs of "heavy tails" [Fig. 3(b)]. Their delta correlatedness holds true [Fig. 3(c)]. Thus, the conditions of the F-test applicability for the Granger causality estimation are satisfied.

Time realizations of the optimal model (10) look very similar to the original time series [Fig. 4(a)]. To compare them quantitatively, Fig. 4(b) shows mean values and 95% intervals of the distributions of the model values $T(t)$ computed from an ensemble of 100 simulated time realizations. The original time series does not come out of the intervals most of the time, i.e., the model quality is sufficiently high. However, this is violated for the GST values in 2001–2005. Thus, one may suspect that the model (10) with constant parameters and constant σ_ξ^2 is not completely adequate, e.g., it may not take into account some factors determining the essential GST rise over the last years.

The hypothesis finds further confirmation under a stricter test. We check whether a univariate model fitted to the interval [1856–1985] can predict the GST rise over the next interval [1985–2005]. The results of model fitting are similar to that for the interval [1856–2005]. Coefficient estimates differ slightly: $a_0=-0.01\pm0.16$ K, $a_1=0.56\pm0.09$, $a_2=0.05\pm0.10$, $a_3=0.02\pm0.10$, and $a_4=0.29\pm0.09$. Prediction error variance is again $\sigma_\xi^2=0.01$ K^2 but the sample variance of GST is smaller $\sigma_T^2=0.03$ K^2. Therefore, the model does not explain 34% of the GST variance. The original GST

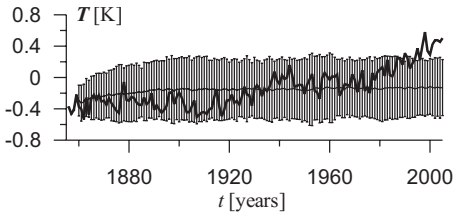

FIG. 5. Behavior of the model (10) fitted to the interval [1856–1985]: mean values (thin line) and 95% intervals (error bars) with the superimposed original data for GST (the thick line).

values over the last 16 years do not fall within the model 95% interval (Fig. 5). Thus, one may assume that something has changed in the GST dynamics in the last two decades, e.g., as a result of external influences.

This is analyzed below with bivariate and multivariate models for GST. All the models are constructed with $d_T=4$. The values of $d_{I\to T}$, $d_{V\to T}$, $d_{n\to T}$, and $\Delta_{I\to T}$, $\Delta_{V\to T}$, and $\Delta_{n\to T}$ are selected to provide the largest prediction improvement and qualitative similarity between the model behavior and the original GST data.

C. GST models including solar activity

An optimal choice of parameters is $d_{I\to T}=1$ and $\Delta_{I\to T}=0$. The influence $I\to T$ is most clearly seen when the interval [1856–1985] is used for model fitting [Fig. 6(a)]. The optimal model reads as

$$T(t)=a_0+a_1T(t-1)+a_4T(t-4)+b_II(t-1)+\eta(t), \tag{11}$$

where $a_0=-93.7\pm44.4$ K, $a_1=0.52\pm0.09$, $a_4=0.27\pm0.09$, and $b_I=0.07\pm0.03$ K/(W/m^2). $G_{I\to T}/\sigma_\xi^2=0.028$ and its

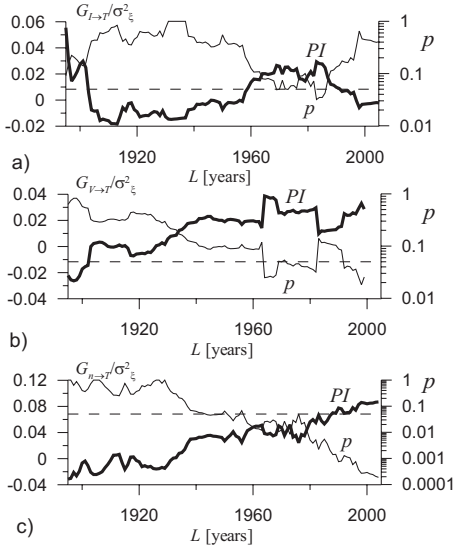

FIG. 6. Bivariate modeling of the GST from different time intervals [1856−L]: (a) model (11) with solar activity; (b) model (12) with volcanic activity; (c) model (13) with CO_2 atmospheric content. The normalized values of the prediction improvement (the thick lines) are indicated on the left y axes (dimensionless); significance levels (the thin lines) on the right y axes (dimensionless). The dashed lines show the level of $p=0.05$.

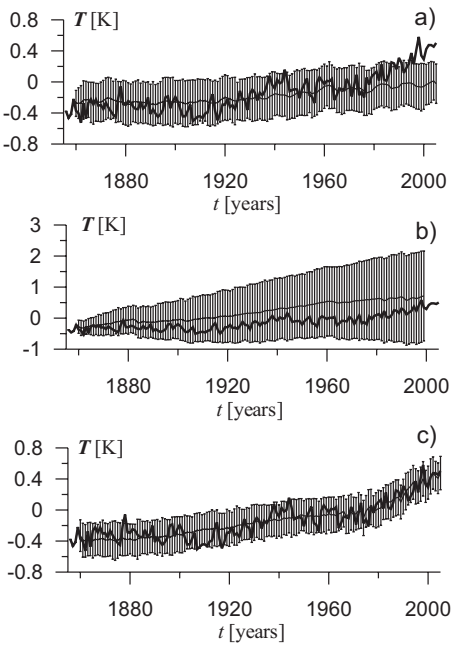

FIG. 7. The original GST values (the thick line) and 95% intervals for the bivariate models of GST: (a) a model (11) with solar activity fitted to the interval [1856–1985]; a model (12) with volcanic activity fitted to the interval [1856–1999]; (c) a model (13) with CO_2 atmospheric content fitted to the interval [1856–2005].

positivity is statistically significant at $p<0.035$. If a model is fitted to the interval [1856–2005], one does not detect any $I\to T$ influence significant at $p<0.05$. It may evidence that the impact of other factors has increased in [1985–2005]. Simulations with the model (11) confirm this assumption indirectly. Figure 7(a) shows an ensemble of simulated realizations under C_0. The 95% intervals are narrower than for the univariate model (Fig. 5), i.e., incorporation of the variable I into the model allows better description of GST in 1856–1985. However, the GST rise in 1985–2005 is not predicted as well.

To assess the long-term effect of the solar activity trend, we simulated an ensemble of time realizations of the model (11) when a detrended signal $I(t)$ taken from [49] is used as input. The result is visually indistinguishable from the plot in Fig. 7(a) (not shown). Thus, the removal of the solar activity trend does not affect the model GST values. Quantitatively, one gets almost the same values $\langle T_{2005}|C_0\rangle=-0.01\pm0.02$ K and $\langle T_{2005}|\text{removed trend}\rangle=0.01\pm0.02$ K. Besides, angular coefficients are close to zero in both cases: $\langle\alpha_{1985-2005}|C_0\rangle\approx\langle\alpha_{1985-2005}|\text{removed trend}\rangle=0.002$ K/year, their positivity is not statistically significant at $p<0.05$. The original trend $\hat{\alpha}_{1985-2005}=0.02$ K/year is not explained by the bivariate model (11). Despite the solar activity influence on the GST is detected with the Granger causality, the long-term causality analysis suggests that the solar activity is not the cause of the GST rise in the last decades.

Incorporation of nonlinear terms into the model does not improve predictions. Therefore, the linear models are optimal. This is the case for all the considerations below as well. Therefore, the results are presented only for the linear models.

D. GST models including volcanic activity

Influence of the volcanic activity appears of the same order of magnitude as that of the solar activity. An optimal choice is $d_{V\to T}=1$ and $\Delta_{V\to T}=-1$, i.e., a model

$$T(t)=a_0+a_1T(t-1)+a_4T(t-4)+b_VV(t)+\eta(t). \quad (12)$$

The influence is detected most clearly from the entire interval [1856–1999] of available data for $V(t)$ [Fig. 6(b)]. $G_{V\to T}/\sigma_\xi^2=0.029$ for that interval and its positivity is statistically significant at $p<0.03$. Model coefficients are $a_0=0.25\pm0.14$ K, $a_1=0.55\pm0.08$, $a_4=0.29\pm0.08$, and $b_V=-0.92\pm0.41$ K.

However, even allowing for the volcanic activity in the AR model, one predicts just big fluctuations of GST about the mean value of $\langle T_{1999}|C_0\rangle=0.7$ K [Fig. 7(b)]. There is no trend in model GST values over the last 20 years: $\langle\alpha_{1985-2000}|C_0\rangle=0.001$ K/year which does not differ from zero significantly [53]. If a signal $V(t)=0$ is used as input then the model predicts even greater values of GST: $\langle T_{1999}|V(t)=0\rangle=1.5$ K. Thus, the long-term effect of volcanic eruptions consists in limiting the GST values. Volcanic activity is relatively high in 1965–1995 [Fig. 2(c)] that should lead to the decrease in GST. Therefore, to explain the GST rise during the last decades as a result of the volcanic activity influence is also impossible.

E. GST models including CO_2 concentration

An optimal choice is $d_{n\to T}=1$ and $\Delta_{n\to T}=0$. Apart from the highly significant prediction improvement, the model behavior is qualitatively similar to the original data (in contrast to $d_{n\to T}>1$). This model reads as

$$T(t)=a_0+a_1T(t-1)+a_4T(t-4)+b_nn(t-1)+\eta(t). \quad (13)$$

Influence of CO_2 appears much more considerable than that of other factors. It is detected most clearly from the entire interval [1856–2005] [Fig. 6(c)]: $G_{n\to T}/\sigma_\xi^2=0.087$ and its positivity is significant at $p<0.000\,2$; the model coefficients are $a_0=-1.10\pm0.29$ K, $a_1=0.46\pm0.08$, $a_4=0.20\pm0.08$, and $b_n=0.003\pm0.001$ K/ppm.

An ensemble of time realizations [Fig. 7(c)] shows that the model (13) under the original conditions C_0 describes the original data more accurately than the models with solar or volcanic activity. Moreover, the model (13) fitted to a narrower interval, e.g., [1856–1960], exhibits practically the same realizations as in Fig. 7(c), i.e., correctly predicts the GST rise despite the data over an interval [1960–2005] are not used for the model fitting. The model (13) fitted to any interval [1856–L] with $L>1935$ produces almost the same behavior. The plots are not shown since they are similar to that for the multivariate AR model presented below.

The long-term effect of $n(t)$ is estimated as follows. If a signal $n(t)=\text{const}=n(1856)$ is used as an input to the model (13) fitted to the interval [1856–1985], one observes just fluctuations of GST about the level of T_{1856} rather than any trend. The long-term effect is $\langle T_{2005}|C_0\rangle-\langle T_{2005}|n(t)=n(1856)\rangle=0.8$ K, $\langle\alpha_{1985-2005}|C_0\rangle-\langle\alpha_{1985-2005}|n(t)=n(1856)\rangle=0.017-0=0.017$ K/year. Thus, according to the model (13), it is the rise in the CO_2 atmospheric content which explains a major part of the recent GST increase.

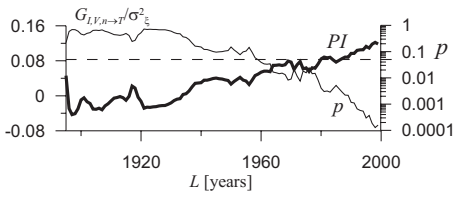

FIG. 8. Results of the multivariate modeling (14) versus the end of the time interval L: the numerical values of prediction improvement (the thick lines) are indicated on the left y axis (dimensionless); significance levels (the thin lines) on the right y axis (dimensionless). The dashed line shows the level of $p=0.05$.

F. Multivariate models of GST

Models are constructed with the above optimal parameters $d_{I\to T}=d_{V\to T}=d_{n\to T}=1$, $\Delta_{I\to T}=\Delta_{n\to T}=0$, and $\Delta_{V\to T}=-1$, i.e., in the form

$$T(t)=a_0+a_1T(t-1)+a_4T(t-4)+b_II(t-1)+b_VV(t)+b_nn(t-1)+\eta(t). \quad (14)$$

The total prediction improvement $G_{I,V,n\to T}/\sigma_\xi^2$ versus L is shown in Fig. 8. It is significant at $p<0.05$ for $1960\le L\le1999$.

Figure 9 presents model coefficients corresponding to different factors. Influences of all three factors can be seen to a certain extent, e.g., for the interval [1856–1985]: $a_0=-62\pm45$ K, $a_1=0.45\pm0.09$, $a_4=0.22\pm0.09$, $b_I=0.045\pm0.033$ K/(W/m^2), $b_V=-0.77\pm0.45$ K, and b_n

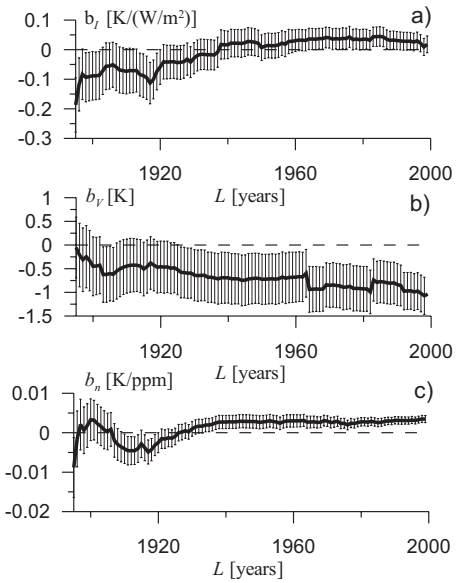

FIG. 9. Coefficients of multivariate model (14) versus the end of the time interval L: (a) b_I corresponds to the solar activity; (b) b_V corresponds to the volcanic activity; (c) b_n corresponds to the CO_2 atmospheric content. Error bars indicate intervals of the ± standard deviation estimate. The dashed lines show the level of 0.

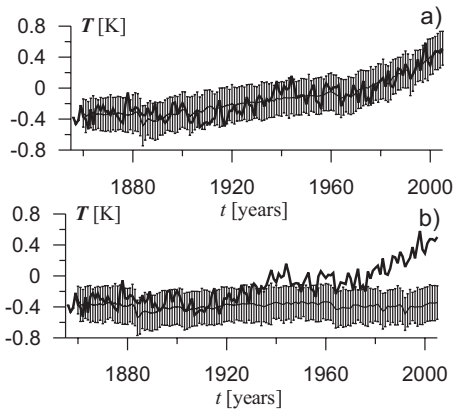

FIG. 10. The original GST time series (the thick lines) and 95% intervals for the model (14) fitted to the interval [1856–1985]: (a) under the original conditions C_0; (b) under the condition $n(t)=n(1856)$.

$=0.002\ 5\pm0.001\ 0$ K/ppm. Then, $G_{I,V,n\to T}/\sigma_\xi^2=0.077$ and its positivity is statistically significant at $p<0.005$, while "bivariate" prediction improvements for the same interval are $G_{I\to T}/\sigma_\xi^2=0.028$, $G_{V\to T}/\sigma_\xi^2=0.012$, and $G_{n\to T}/\sigma_\xi^2=0.053$. Hence, the contribution of CO_2 to the GST dynamics is the strongest one. It becomes even more obvious with the long-term analysis.

The model (14) fitted to the interval [1856–1985] under the condition C_0 exhibits realizations which are very close to the original GST data [Fig. 10(a)]. In particular, it predicts well the GST trend in the last years: $\langle T_{2005}|C_0\rangle=0.52$ K, $\langle\alpha_{1985-2005}|C_0\rangle=0.015$ K/year. If a detrended signal $I(t)$ or zero volcanic activity is used as inputs, almost nothing changes in the model behavior, i.e., the long-term effect of these two factors is very weak. If a constant value of $n(t)$ at the level of 1856 is used as input, the model does not exhibit the GST rise [Fig. 10(b)]. It gives $\langle T_{2005}|n(t)=n(1856)\rangle=-0.34$ K and a zero trend $\langle\alpha_{1985-2005}|n(t)=n(1856)\rangle$.

Thus, the incorporation of the variable n into the model allows to explain the GST rise in the last years (in particular, at least 75% of the original GST trend $\hat{\alpha}_{1985-2005}=0.02$ K/year) in contrast to the other two factors. This result is observed if any $L>1940$ is used for the model fitting.

To illustrate an impact of CO_2 over a shorter time scale, the interval [1856–1960] is used to fit the model (14). With this model, we check what happens if n stops to increase right after 1960. The original data $n(t)$ for $t\leq1960$ and artificial signal $n(t)=n(1960)$ for $t>1960$ are used as input to the model. Figure 11 shows that a model quantity T stops to

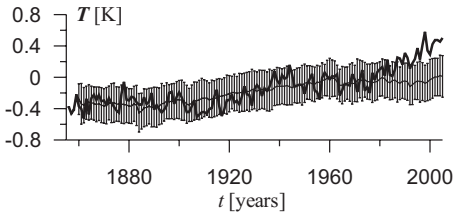

FIG. 11. The original GST data (the thick line) and 95% intervals for the model (14) fitted to the interval [1856–1960] under the condition $n(t)=n(1960)$ for $t>1960$.

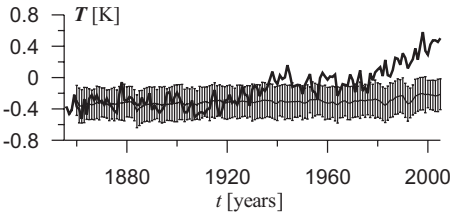

FIG. 12. The original GST data (the thick line) and 95% intervals for the model (14) fitted to the interval [1856–1930] under the original conditions C_0.

rise approximately after 1960, i.e., the changes in $n(t)$ manifest themselves through the dynamics of the GST quite quickly.

The influence $n\to T$ cannot be detected from the intervals with $L<1940$. For example, Fig. 12 shows realizations of the model (14) fitted to the interval [1856–1930]. Using such a short piece of data, one "misses" all the influences on GST. Therefore, the corresponding model does not predict the GST rise even under the original conditions C_0.

In more detail, the long-term characteristics of the model (14) fitted to the interval $[1856-L]$ are presented in Fig. 13 versus L. The plots show quantitatively that $L=1940$ is the least value necessary to reveal the influence $n\to T$.

V. CONCLUSIONS

We have suggested the concept of the long-term causality to characterize long-term effects of couplings between observed processes. Our approach is based on the construction of empirical models and analysis of their behavior under various conditions. It complements the widely used Granger causality which assesses short-term effects of coupling.

Although the Granger causality remains a basic tool to *detect* causal influences, the proposed characteristics are more appropriate to quantify the strength and importance of those influences. With several mathematical examples, we

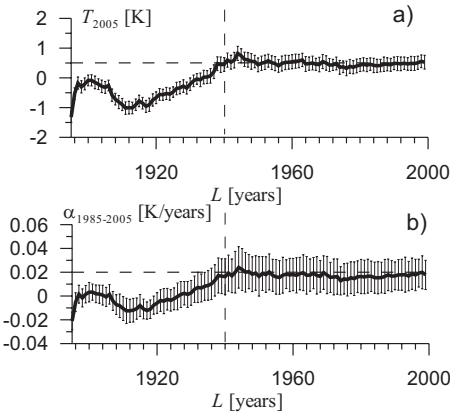

FIG. 13. Long-term characteristics of the model (14) fitted to the intervals $[1856-L]$ versus L under the original conditions C_0: (a) T_{2005}; (b) $\alpha_{1985-2005}$. Error bars show 95% intervals of the distributions. Horizontal dashed lines show characteristics of the original data. Vertical dashed lines indicate the value of L where the model characteristics get close to the original ones.

have shown that the Granger causality may not distinguish between the situations where an external driving determines the entire qualitative character of an observed process and where it induces only weak quantitative perturbations. Furthermore, the Granger causality often underestimates the importance of an influence since a univariate model for a driven process implicitly describes the driving process as well. The long-term causality allows proper characterization of all these situations under the assumption that an empirical model structure is appropriate to describe the observed process under various conditions.

Both Granger causality and long-term causality are used to estimate an effect of solar activity, volcanic activity, and carbon dioxide atmospheric content on the global surface temperature. The Granger causality shows that the three factors determine about 10% of the quantity σ_ξ^2 which is a variance of the short-term GST fluctuations unexplained by univariate models. The short-term impact of CO_2 is several times stronger than the impacts of the other two factors. The long-term causality reveals that the CO_2 content is a determinative factor of the GST rise in the last decades. Thus, according to the empirical models, the increase in the CO_2 concentration determines at least 75% of the GST trend in 1985–2005, while the other two factors are not the causes of the global warming. In particular, if the CO_2 concentration remained at the level of 1856 year, the GST would not rise during the last century. In contrast, variations in solar and volcanic activities would not lead to significant changes in the GST trend. All the influences are detected reliably if the data at least over the interval [1856–1940] are used for the model fitting.

ACKNOWLEDGMENTS

The work is supported by the Russian Foundation for Basic Research (Grants No. 07-05-00381 and No. 08-05-00532) and Programs of RAS and Ministry of Education and Science RF.

[1] A. Pikovsky, M. Rosenblum, and J. Kurths, *Synchronization: A Universal Concept in Nonlinear Sciences* (Cambridge University Press, Cambridge, New York, 2001).
[2] B. Bezruchko, V. Ponomarenko, M. G. Rosenblum, and A. S. Pikovsky, Chaos **13**, 179 (2003).
[3] W. Wang, B. T. Anderson, R. K. Kaufmann, and R. B. Myneni, J. Clim. **17**, 4752 (2004).
[4] D. Maraun and J. Kurths, Geophys. Res. Lett. **32**, L15709 (2005).
[5] I. I. Mokhov, V. A. Bezverkhny, and A. A. Karpenko, Izv., Acad. Sci., USSR, Atmos. Oceanic Phys. **41**, 523 (2005).
[6] P. F. Verdes, Phys. Rev. E **72**, 026222 (2005).
[7] M. Palus and D. Novotna, Nonlinear Processes Geophys. **13**, 287 (2006).
[8] I. I. Mokhov and D. A. Smirnov, Geophys. Res. Lett. **33**, L03708 (2006).
[9] T. J. Mosedale, D. B. Stephenson, M. Collins, and T. C. Mills, J. Clim. **19**, 1182 (2006).
[10] J. Moore, A. Grinsted, and S. Jevrejeva, Geophys. Res. Lett. **33**, L17705 (2006).
[11] I. I. Mokhov and D. A. Smirnov, Izv., Acad. Sci., USSR, Atmos. Oceanic Phys. **44**, 263 (2008).
[12] P. A. Tass, *Phase Resetting in Medicine and Biology* (Springer-Verlag, Berlin, 1999).
[13] P. A. Tass, M. G. Rosenblum, J. Weule, J. Kurths, A. Pikovsky, J. Volkmann, A. Schnitzler, and H.-J. Freund, Phys. Rev. Lett. **81**, 3291 (1998).
[14] S. J. Schiff, P. So, T. Chang, R. E. Burke, and T. Sauer, Phys. Rev. E **54**, 6708 (1996).
[15] J. Arnhold, K. Lehnertz, P. Grassberger, and C. E. Elger, Physica D **134**, 419 (1999).
[16] M. Le Van Quyen, J. Martinerie, C. Adam, and F. Varela, Physica D **127**, 250 (1999).
[17] F. Mormann, K. Lehnertz, P. David, and C. E. Elger, Physica D **144**, 358 (2000).
[18] K. J. Friston, L. Harrison, and W. Penny, Neuroimage **19**, 1273 (2003).
[19] T. Kiemel, K. Gormley, L. Guan, T. Williams, and A. Cohen, J. Comput. Neurosci. **15**, 233 (2003).
[20] E. Pereda, R. Quian Quiroga, and J. Bhattacharya, Prog. Neurobiol. **77**, 1 (2005).
[21] D. A. Smirnov, M. B. Bodrov, J. L. Perez Velazquez, R. A. Wennberg, and B. P. Bezruchko, Chaos **15**, 024102 (2005).
[22] J. Brea, D. F. Russell, and A. B. Neiman, Chaos **16**, 026111 (2006).
[23] B. Schelter, M. Winterhalder, M. Eichler, M. Peifer, B. Hellwig, B. Guschlbauer, C. Luecking, R. Dahlhaus, and J. Timmer, J. Neurosci. Methods **152**, 210 (2006).
[24] T. Kreuz, F. Mormann, R. G. Andrzejak, A. Kraskov, K. Lehnertz, and P. Grassberger, Physica D **225**, 29 (2007).
[25] H. Osterhage, F. Mormann, T. Wagner, and K. Lehnertz, Int. J. Neural Syst. **17**, 139 (2007).
[26] M. Staniek and K. Lehnertz, Phys. Rev. Lett. **100**, 158101 (2008).
[27] J. Prusseit and K. Lehnertz, Phys. Rev. E **77**, 041914 (2008).
[28] L. Faes, A. Porta, and G. Nollo, Phys. Rev. E **78**, 026201 (2008).
[29] D. Smirnov, U. B. Barnikol, T. T. Barnikol, B. P. Bezruchko, C. Hauptmann, C. Buehrle, M. Maarouf, V. Sturm, H.-J. Freund, and P. A. Tass, EPL **83**, 20003 (2008).
[30] E. Sitnikova, T. Dikanev, D. Smirnov, B. Bezruchko, and G. van Luijtelaar, J. Neurosci. Methods **170**, 245 (2008).
[31] S. Boccaletti, J. Kurths, G. Osipov, D. Valladares, and C. Zhou, Phys. Rep. **366**, 1 (2002).
[32] M. D. Prokhorov, V. I. Ponomarenko, V. I. Gridnev, M. B. Bodrov, and A. B. Bespyatov, Phys. Rev. E **68**, 041913 (2003).
[33] C. W. J. Granger, Econometrica **37**, 424 (1969).
[34] M. C. Romano, M. Thiel, J. Kurths, and C. Grebogi, Phys. Rev. E **76**, 036211 (2007).
[35] R. Andrzejak, A. Ledberg, and G. Deco, New J. Phys. **8**, 6 (2006).

[36] M. Palus and M. Vejmelka, Phys. Rev. E **75**, 056211 (2007).
[37] T. Schreiber, Phys. Rev. Lett. **85**, 461 (2000).
[38] K. Hlavackova-Schindler, M. Palus, M. Vejmelka, and J. Bhattacharya, Phys. Rep. **441**, 1 (2007).
[39] M. Vejmelka and M. Palus, Phys. Rev. E **77**, 026214 (2008).
[40] N. Ancona, D. Marinazzo, and S. Stramaglia, Phys. Rev. E **70**, 056221 (2004).
[41] U. Feldmann and J. Bhattacharya, Int. J. Bifurcation Chaos Appl. Sci. Eng. **14**, 505 (2004).
[42] P. A. Tass, Biol. Cybern. **89**, 81 (2003).
[43] C. Change, in *The Physical Science Basis*, edited by S. Solomon *et al.* (Cambridge University Press, Cambridge, New York, 2007).
[44] H. Akaike, IEEE Trans. Autom. Control **19**, 716 (1974).
[45] G. Schwartz, Ann. Stat. **6**, 461 (1978).
[46] Uniform distribution of ξ is used in the example (6) since almost any realization of x_1 would diverge to infinity for Gaussian noise.
[47] Moreover, one can assess not only a "separate" influence $j \to k$ but also a "combined" influence by imposing a condition C on several processes.
[48] I. I. Mokhov, V. A. Bezerkhny, A. V. Eliseev, and A. A. Karpenko, Dokl. Akad. Nauk **409**, 1 (2006).
[49] J. Lean, G. Rottman, J. Harder, and G. Kopp, Sol. Phys. **230**, 27 (2005).
[50] Climate Research Unit (University of East Anglia) (http://www.cru.uea.ac.uk).
[51] M. Sato, J. E. Hansen, M. P. McCormick, and J. B. Pollack, J. Geophys. Res. **98**, 22987 (1993).
[52] T. J. Conway, P. P. Tans, L. S. Waterman, K. W. Thoning, D. R. Kitziis, K. A. Masarie, and N. Zhang, J. Geophys. Res. **99**, 22831 (1994).
[53] To simulate the model values of T in 2000–2005 under the condition C_0, the time series $V(t)$ is expanded with the values $V(t)=0$ in 2000–2005 which are close to $V(1999)$. These lowest possible values may somewhat overestimate the model values of T in 2000–2005. Nevertheless, it appears that even with them the model (12) fails to describe the GST trend in the recent decades.